UNIVERSITY OF AMSTERDAM

UvA-DARE (Digital Academic Repository)

Cationic Copper Iminophosphorane Complexes as CuAAC Catalysts: A Mechanistic Study

Venderbosch, B.; Oudsen, J.-P.H.; van der Vlugt, J.I.; Korstanje, T.J.; Tromp, M.

DOI
10.1021/acs.organomet.0c00348

Publication date
2020

Document Version
Final published version

Published in
Organometallics

License
CC BY-NC-ND

Link to publication

Citation for published version (APA):
Venderbosch, B., Oudsen, J-PH., van der Vlugt, J. I., Korstanje, T. J., & Tromp, M. (2020). Cationic Copper Iminophosphorane Complexes as CuAAC Catalysts: A Mechanistic Study. *Organometallics*, *39*(19), 3480-3489. https://doi.org/10.1021/acs.organomet.0c00348

General rights
It is not permitted to download or to forward/distribute the text or part of it without the consent of the author(s) and/or copyright holder(s), other than for strictly personal, individual use, unless the work is under an open content license (like Creative Commons).

Disclaimer/Complaints regulations
If you believe that digital publication of certain material infringes any of your rights or (privacy) interests, please let the Library know, stating your reasons. In case of a legitimate complaint, the Library will make the material inaccessible and/or remove it from the website. Please Ask the Library: https://uba.uva.nl/en/contact, or a letter to: Library of the University of Amsterdam, Secretariat, Singel 425, 1012 WP Amsterdam, The Netherlands. You will be contacted as soon as possible.

UvA-DARE is a service provided by the library of the University of Amsterdam (https://dare.uva.nl)

Download date:26 Jul 2022

This is an open access article published under a Creative Commons Non-Commercial No Derivative Works (CC-BY-NC-ND) Attribution License, which permits copying and redistribution of the article, and creation of adaptations, all for non-commercial purposes.

ACS AUTHORCHOICE

ORGANOMETALLICS

pubs.acs.org/Organometallics

Article

Cationic Copper Iminophosphorane Complexes as CuAAC Catalysts: A Mechanistic Study

Bas Venderbosch, Jean-Pierre H. Oudsen, Jarl Ivar van der Vlugt, Ties J. Korstanje, and Moniek Tromp*

Cite This: *Organometallics* 2020, 39, 3480−3489

Read Online

ACCESS | Metrics & More | Article Recommendations | Supporting Information

ABSTRACT: We have combined Cu K-edge X-ray absorption spectroscopy with NMR spectroscopy (^{1}H and ^{31}P) to study the Cu-catalyzed azide−alkyne cycloaddition (CuAAC) reaction under *operando* conditions. A variety of novel, well-defined Cu^{I} iminophosphorane complexes were prepared. These ligands, based on the *in situ* Staudinger reduction when $[Cu(PPh_3)_3Br]$ is employed, were found to be active catalysts in the CuAAC reaction. Here, we highlight recent advances in mechanistic understanding of the CuAAC reaction using spectroscopic and kinetic investigations under strict air-free and *operando* conditions. A mononuclear Cu triazolide intermediate is identified to be the resting state during catalysis; cyclization and protonation both have an effect on the rate of the reaction. A key finding of this study includes a novel group of highly modular Cu^{I} complexes that are active in the base-free CuAAC reaction.

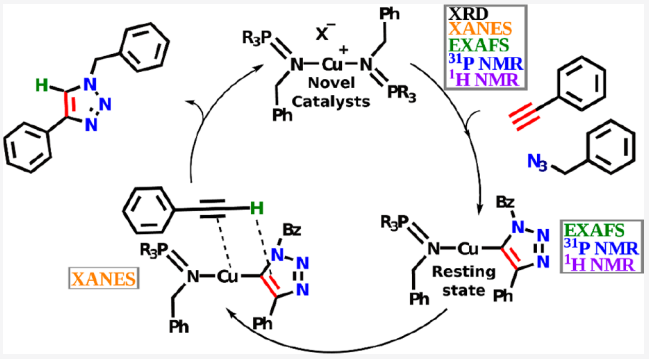

INTRODUCTION

The Cu^{I}-catalyzed azide−alkyne cycloaddition (CuAAC) reaction is a valuable methodology to generate triazoles, a common scaffold in complex drug molecules.[1,2] The uncatalyzed variant of this reaction (a.k.a. Huisgen 1,3-dipolar cycloaddition) yields a mixture of 1,4- and 1,5-regioisomers of the targeted triazole, and the reaction requires elevated temperature (Scheme 1a).[3] On the contrary, the Cu-catalyzed version yields solely the 1,4-regioisomer and is typically performed at room temperature (Scheme 1b).[4,5] Because of the high yields, selectivity, and robustness of the CuAAC reaction, it is a prime example of a so-called click reaction.[6] The active CuAAC catalyst is often generated *in situ* by reduction of a Cu^{II} precursor.[7] Alternatively, catalysis can be performed directly with a preformed Cu^{I} complex ligated by, for example, carbenes,[8] amines,[9] or phosphines.[10]

Several mechanistic studies have been performed on the CuAAC reaction. An early proposal made by Sharpless and co-workers suggested that catalysis proceeds via mononuclear Cu^{I} intermediates.[5] Later mechanistic studies, however, revealed a second-order rate dependency on the concentration of Cu^{I}.[11] DFT calculations show a decrease in the activation barrier when a second Cu atom is introduced.[12] In addition, various isolable polynuclear copper acetylide complexes were found to be catalytically active in the CuAAC reaction.[13−16] Based on these observations, catalysis is believed to proceed through dinuclear Cu^{I} intermediates (Scheme 1c).

Most of these mechanistic proposals are based on either solid-state structures, obtained through single-crystal X-ray diffraction (XRD), or DFT calculations performed in the gas phase. To date, limited spectroscopic studies have been performed under *operando* conditions. Dinuclear intermediates have recently been detected using electrospray ionization (ESI) mass spectrometry (MS) under catalytic conditions.[17] The CuAAC reaction was also studied by using infrared spectroscopy (IR) by Wu et al.,[18] and the rate-determining step was identified to be the cyclization of the azide and alkyne. However, no conclusions were made regarding the exact structure or the nuclearity of the active species.

This study provides more insights into the mechanism of the CuAAC reaction by using novel, cationic, homoleptic Cu^{I} iminophosphorane complexes. The mechanism of the CuAAC reaction catalyzed by these iminophosphorane-stabilized Cu^{I} complexes is investigated by using *operando* spectroscopy (NMR and Cu K-edge XAS) and kinetic experiments. Additionally, a mononuclear Cu^{I} triazolide complex is prepared, and its relevance to the catalytic cycle is investigated. The DFT results support protonation of the Cu^{I} triazolide to be the rate-determining step in the catalytic cycle.

Received: May 18, 2020
Published: September 30, 2020

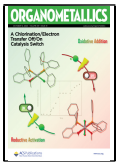

Downloaded via UNIV AMSTERDAM on February 4, 2021 at 10:51:25 (UTC).
See https://pubs.acs.org/sharingguidelines for options on how to legitimately share published articles.

Scheme 1. (a) Uncatalyzed Azide−Alkyne Cycloaddition Reaction to Yield the 1,4- and 1,5-Regioisomer of the Target Triazole; (b) Cu^{I}-Catalyzed Azide−Alkyne Cycloaddition Reaction to Yield Solely the 1,5-Regioisomer; (c) Recent Mechanistic Proposal for the Cu^{I}-Catalyzed Azide−Alkyne Cycloaddition Reaction, Involving Dinuclear Cu^{I} Intermediates[a]

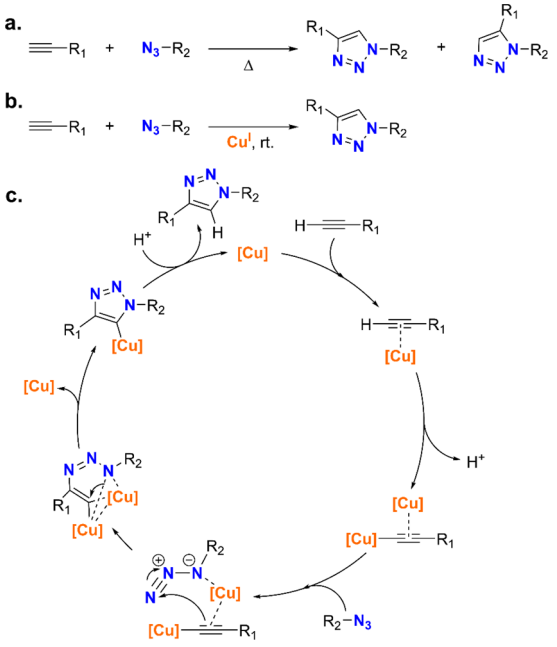

[a]This cycle is based on the proposal made in ref 13.

RESULTS AND DISCUSSION

Degradation of $[Cu(PPh_3)_3Br]$ under Catalytic Conditions. Initially, $[Cu(PPh_3)_3Br]$ was selected for this mechanistic study. The use of $[Cu(PPh_3)_3Br]$ as a potent, organic-soluble CuAAC catalyst was first reported by Pérez-Balderas et al.[19] Later, Lal et al. increased the applicability of the catalyst and showed that the catalyst can also operate in water and under neat conditions.[20] The catalyst has also shown application in the field of click polymerization.[21,22]

In this study, reactions were performed under strict air-free conditions to prevent oxygen or moisture affecting the course of the reaction. As a model system, the reaction between benzyl azide and phenylacetylene in the presence of $[Cu(PPh_3)_3Br]$ in THF-d_8 was monitored by using ^{1}H NMR spectroscopy (Figure 1, left).[23] The conversion was determined from the ^{1}H spectra by comparing the amount of benzyl azide relative to the amount of product triazole (Supporting Information, section 1.5).

After roughly 15 h a conversion of ∼75% is obtained. Interestingly, an induction period is present, as can be seen in the inset of Figure 1, suggestive of structural changes occurring to the complex prior to formation of the active catalyst. Monitoring this system in time using ^{31}P NMR spectroscopy was used to shed light on the origin of this induction period (Figure 1, right). Two distinct resonances are observed over the course of hours. First, a resonance is present at around δ_P = −6 ppm that decreases in time. This resonance is assigned to PPh_3, either bound or free in solution. The second resonance increases in time at around δ_P = 10 ppm.

The broadness of the observed resonances is indicative of underlying dynamic processes. These processes were slowed by cooling the reaction mixture to −60 °C; multiple novel resonances were identified (Figure S119). One of these resonances (δ_P = 6.4 ppm) is attributed to the product of the Staudinger reaction between benzyl azide and PPh_3, indicating that the phosphine ligands undergo oxidation under catalytic conditions.

Synthesis and Characterization of Cu Iminophosphorane Complexes. The Staudinger reaction occurring under catalytic azide−alkyne coupling conditions in the presence of air and moisture has already been observed with $[Cu(PPh_3)_3Br]$ and was considered an unwanted reaction.[24,25] However, our results imply that the Staudinger reaction is relevant to generate the catalytically active species from $[Cu(PPh_3)_3Br]$ under anhydrous and oxygen-free conditions. These combined results suggest that iminophosphorane (IP) ligation to copper might be of prime importance in this activation process to enable the CuAAC reaction. Notably, copper complexes with chelating IP-based ligands have previously been employed in the CuAAC reaction.[26,27]

To investigate the coordination chemistry of monodentate IPs, we prepared a variety of IPs (Scheme 2) by mixing the respective phosphine and benzyl azide in a suitable solvent (either toluene or THF). For the less sterically encumbered IPs ($\mathbf{L1_H}$, $\mathbf{L2_{OMe}}$, $\mathbf{L3_{Cl}}$ and $\mathbf{L5_{Me}}$) the reaction readily proceeds at room temperature, indicated by rapid N_2 evolution. Formation of $\mathbf{L4_{Cy}}$ required heating to 110 °C, presumably due to steric hindrance imposed by PCy_3, hampering elimination of N_2 from the phosphazide intermediate. $\mathbf{L1_H}$,

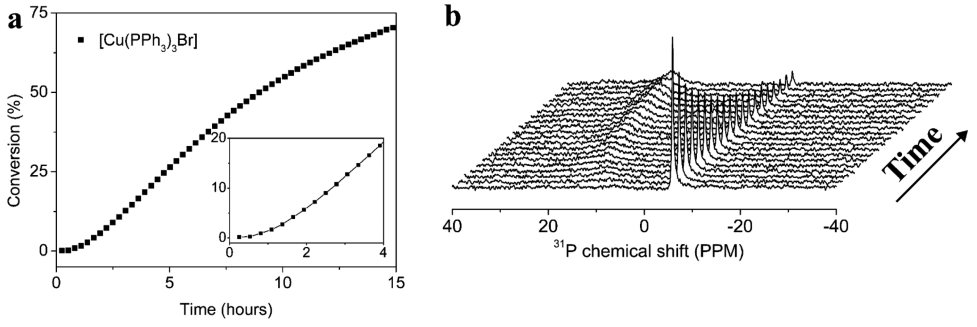

Figure 1. Reaction between benzyl azide (1 equiv) and phenylacetylene (1.2 equiv) in the presence of $[Cu(PPh_3)_3Br]$ (2.5 mol %) in THF-d_8. (a) Conversion followed by ^{1}H NMR spectroscopy. (b) Temporal evolution of the resonances observed in the ^{31}P NMR spectrum. Conversion was determined by comparing the integral of the benzyl azide and triazole moiety. In the ^{31}P NMR spectrum, the first spectrum is measured after 15 min and time intervals of 15 min are employed between consecutive spectra.

https://dx.doi.org/10.1021/acs.organomet.0c00348
Organometallics 2020, 39, 3480−3489

Scheme 2. Staudinger Reaction to Produce the Target Iminophosphorane Ligands L1−L5

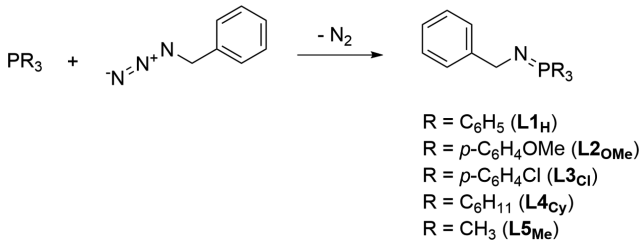

$\mathbf{L2}_{\mathbf{OMe}}$, $\mathbf{L3}_{\mathbf{Cl}}$, and $\mathbf{L4}_{\mathbf{Cy}}$ were isolated as white solids, whereas $\mathbf{L5}_{\mathbf{Me}}$ was obtained as a pink liquid. The ^{1}H NMR spectrum of each IP shows a characteristic doublet ($^3J_{P-H}$) for the benzylic hydrogens. In addition, the observed ^{31}P NMR resonance for the respective P═N moiety varied depending on the parent phosphine employed. For $\mathbf{L1}_{\mathbf{H}}$, $\mathbf{L2}_{\mathbf{OMe}}$, and $\mathbf{L3}_{\mathbf{Cl}}$ a single resonance was observed with a value of $\delta_P \approx 9$ ppm, while $\mathbf{L4}_{\mathbf{Cy}}$ resonates at δ_P = 24.3 ppm and $\mathbf{L5}_{\mathbf{Me}}$ resonates at δ_P = 11.6 ppm.

Coordination of $\mathbf{L1}_{\mathbf{H}}$ to Cu^I was successfully achieved by reaction of the ligand with CuBr (Supporting Information, section 2.6). Single-crystal X-ray diffraction revealed a homoleptic complex of the structure $[Cu(\mathbf{L1}_{\mathbf{H}})_2][CuBr_2]$. The $[CuBr_2]^-$ anion can also participate in the CuAAC reaction, as $NBu_4[CuBr_2]$ (2.5 mol % in THF-d_8) showed moderate activity in the CuAAC reaction (34% conversion after 22 h). To prevent the participation of the cuprate anion in the CuAAC reaction, we used $[Cu(NCMe)_4]BF_4$ as the Cu^I source. Through reaction of ligand **L1−L5** (2.1 equiv) with $[Cu(NCMe)_4]BF_4$ (Scheme 3), complexes **1−5** with the

Scheme 3. Synthesis of Cu Iminophosphorane Complexes 1−5

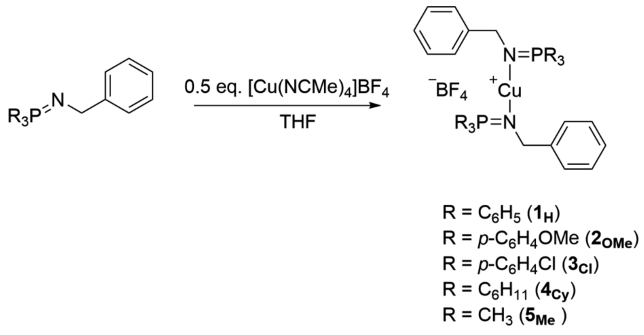

general structure $[Cu(IP)_2]BF_4$ were successfully synthesized and were fully characterized with NMR spectroscopy, mass spectrometry (MS), and in most cases single-crystal X-ray diffraction.

Using cold-spray ionization (CSI) MS, we detected only the homoleptic cationic fragments, with no noticeable fragmentation of these complexes. NMR spectroscopy shows clear changes in the ^{31}P NMR resonances for the corresponding complexes compared to the free ligands (see the Experimental Section) with $\Delta\delta$ of ∼24 ppm in the case of aromatic substituents and $\Delta\delta$ of ∼36 ppm in the case of aliphatic substituents on the phosphine. Interestingly, no broadening of the ^{31}P NMR resonances for any of the $[Cu(IP)_2]BF_4$ complexes was observed at room temperature. In addition, a shift in the ^{1}H NMR spectrum for the benzylic hydrogens is observed upon coordination to copper for each complex.

Single crystals suitable for X-ray diffraction for complexes $\mathbf{1}_{\mathbf{H}}$ (as the PF_6 complex) and $\mathbf{2}_{\mathbf{OMe}}$, $\mathbf{3}_{\mathbf{Cl}}$, and $\mathbf{4}_{\mathbf{Cy}}$ were obtained by diffusion of pentane into a saturated THF solution of the respective complex (Figure 2). Complex $\mathbf{5}_{\mathbf{Me}}$ proved very sensitive, with a color change (from white to yellow) of the solid material observed inside an Ar-filled glovebox in the course of several days, presumably hampering the isolation of single crystals for this complex.

All four molecular structures show a linear coordination geometry around Cu, with N−Cu−N angles close to 180°. The largest deviation from linearity is observed for complex $\mathbf{4}_{\mathbf{Cy}}$ (∠N−Cu−N 174.86°), presumably arising from the steric bulk introduced by the PCy_3 substituents. The coordination environment around the nitrogen atoms is close to trigonal planar in each case, and the Cu−N distances vary only slightly (between 1.87 and 1.90 Å).

Catalytic Performance of the Prepared Cu Iminophosphorane Complexes. The catalytic performance of the complexes (**1−5**) in the CuAAC reaction between phenylacetylene (1.2 equiv) and benzyl azide (1 equiv) in THF-d_8 was monitored over the course of 15 h by using ^{1}H NMR spectroscopy (Figure 3). All complexes were found to be active in the CuAAC reaction, but a large variation for their performance in the CuAAC reaction is observed. A side-by-side comparison of complexes $\mathbf{1}_{\mathbf{H}}$, $\mathbf{2}_{\mathbf{OMe}}$, and $\mathbf{3}_{\mathbf{Cl}}$ may provide insight into the influence of the electronic structure of the ligand on the catalytic activity in the CuAAC reaction (Figure 3, left). The observed activity trend is $\mathbf{3}_{\mathbf{Cl}} > \mathbf{1}_{\mathbf{H}} > \mathbf{2}_{\mathbf{OMe}}$, which suggests that a decrease in Lewis basicity of the ligand leads to enhanced catalytic performance.

A comparison of the catalytic activity of $\mathbf{1}_{\mathbf{H}}$, $\mathbf{4}_{\mathbf{Cy}}$, and $\mathbf{5}_{\mathbf{Me}}$ seems to imply that a reduction of steric bulk is beneficial for catalysis (Figure 3, right). However, analysis of the catalytic performance of $\mathbf{5}_{\mathbf{Me}}$ shows an increase of its catalytic performance with time. This may be related to the small substituents at phosphorus, enabling the triazole product to also ligate to the metal and have a positive influence on the rate of the rate of the reaction (i.e., autocatalysis).[28] This prevented us from relating the catalytic activity to the steric bulk of the ligand.

We also assessed the catalytic performance of $\mathbf{1}_{\mathbf{H}}$ under ambient conditions (Supporting Information, section 4.11). The catalytic performance under ambient conditions is greatly enhanced. The origin of this effect is unknown, but likely protonation will be more facile (*vide infra*).

Mechanistic Study of the CuAAC Reaction Using Cu Iminophosphorane Complexes. Because of the ease of synthesis and good stability in solution, complex $\mathbf{1}_{\mathbf{H}}$ was used for a mechanistic study. To arrive at potentially relevant catalytic intermediates, initial synthetic attempts focused on a Cu−acetylide species bearing ligand $\mathbf{L1}_{\mathbf{H}}$ as previously isolated mono- and dinuclear Cu−acetylides showed to be relevant active catalytic species.[15] Cu complexes containing an internal base can directly react with alkynes to prepare Cu acetylides. This approach has been used to prepare Cu^I complexes containing carbene ligands.[14,29,30] It is likely that iminophosphorane ligands can also act as internal bases, given their qualification as superbases; the closely related iminophosphorane Ph_3P═NCy was found to have a pK_{BH+} of 22.7 in acetonitrile.[31]

https://dx.doi.org/10.1021/acs.organomet.0c00348
Organometallics 2020, 39, 3480−3489

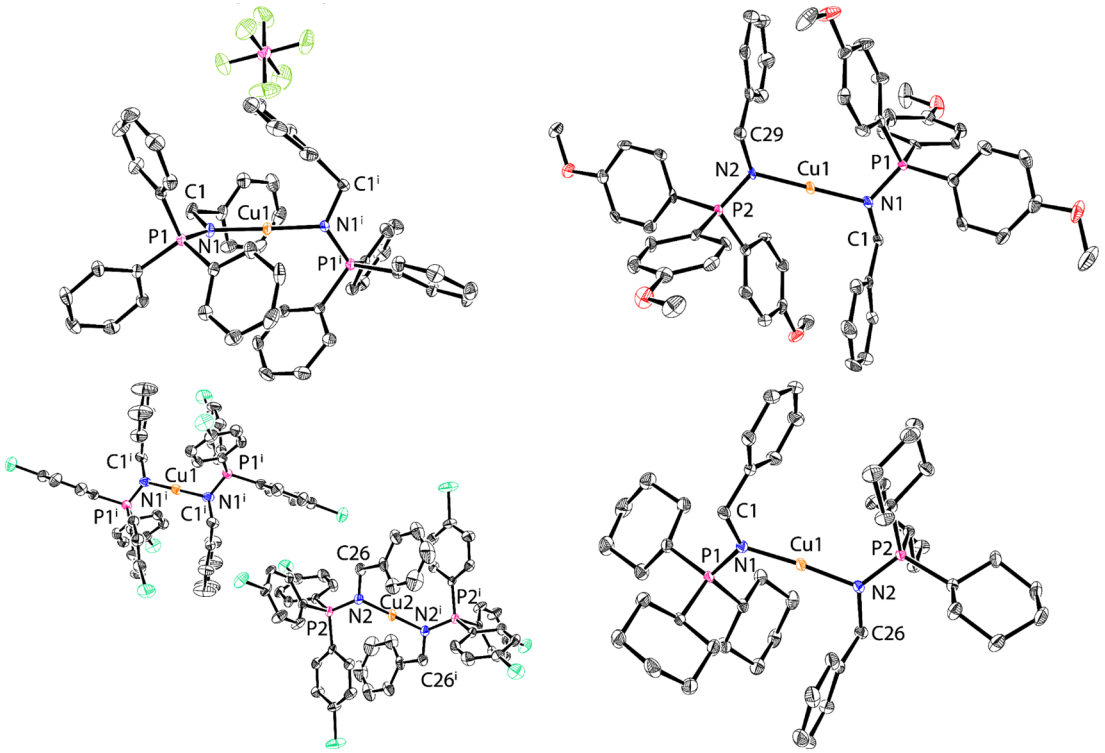

Figure 2. ORTEP plots (50% probability level) for $\mathbf{1_H}$ (as PF_6 salt, top left), $\mathbf{2_{OMe}}$ (top right), $\mathbf{3_{Cl}}$ (bottom left), and $\mathbf{4_{Cy}}$ (bottom right). Hydrogen atoms and anions are omitted for clarity. Selected bond lengths [Å], angles [deg], and torsion angles [deg]: For $\mathbf{1_H}$: $Cu_1–N_1$ 1.8902(18); $N_1–P_1$ 1.6055(18); $N_1–C_1$ 1.487(3); $N_1–Cu_1–N_1^i$ 178.80(11); $P_1–N_1–Cu_1$ 120.18(11); $C_1–N_1–Cu_1$ 117.04(14); $C_1–N_1–P_1$ 120.27(15); $P_1–N_1–N_1^i–P_1^i$ 99.24. For $\mathbf{2_{OMe}}$: $Cu_1–N_1$ 1.879(5); $Cu_1–N_2$ 1.867(5); $N_1–P_1$ 1.600(5); $N_2–P_2$ 1.600(5); $N_1–C_1$ 1.464(8); $N_2–C_{29}$ 1.478(8); $N_1–Cu_1–N_2$ 179.7(3); $P_1–N_1–Cu_1$ 117.3(4); $C_1–N_1–Cu_1$ 117.3(4); $C_1–N_1–P_1$ 121.2(4); $P_2–N_2–Cu_1$ 118.1(3); $C_{29}–N_2–Cu_1$ 117.7(4); $C_{29}–N_2–P_2$ 118.3(4); $P_1–N_1–N_2–P_2$ 176.95. For $\mathbf{3_{Cl}}$: $Cu_1–N_1$ 1.865(4); $N_1–P_1$ 1.592(4); $N_1–C_1$ 1.474(6); $N_1–Cu_1–N_1^i$ 180.0; $P_1–N_1–Cu_1$ 121.5(2); $C_1–N_1–Cu_1$ 116.0(3); $C_1–N_1–P_1$ 119.6(3); $P_1–N_1–N_1^i–P_1^i$ 180.0; $Cu_2–N_2$ 1.860(4); $N_2–P_2$ 1.587(4); $N_2–C_{26}$ 1.472(6); $N_2–Cu_2–N_2^i$ 180.0; $P_2–N_2–Cu_2$ 117.5(2); $C_{26}–N_2–Cu_2$ 121.0(3); $C_{26}–N_2–P_2$ 119.0(3) $P_1–N_1–N_1^i–P_1^i$ 180.0. For $\mathbf{4_{Cy}}$: $Cu_1–N_1$ 1.8796(13); $Cu_1–N_2$ 1.8813(13) $N_1–P_1$ 1.6156(13); $N_2–P_2$ 1.6169(13); $N_1–C_1$ 1.477(2); $N_2–C_{26}$ 1.472(2); $N_1–Cu_1–N_2$ 174.84(6); $P_1–N_1–Cu_1$ 121.83(8); $C_1–N_1–Cu_1$ 113.18(10); $C_1–N_1–P_1$ 120.54(11); $P_2–N_2–Cu_1$ 119.55(7); $C_{26}–N_2–Cu_1$ 118.07(10); $C_{26}–N_2–P_2$ 119.24(10); $P_1–N_1–N_2–P_2$ 144.05.

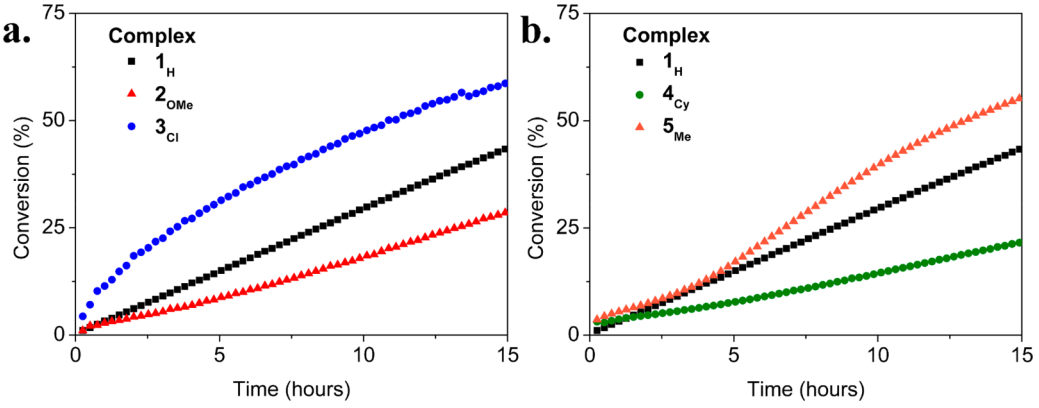

Figure 3. Conversion as a function of time for the various prepared complexes. Reactions were performed by mixing the Cu complex (2.5 mol % with respect to Cu), with benzyl azide (1 equiv) in THF-d_8 (1 mL), followed by the addition of phenylacetylene (1.2 equiv).

The hypothesis that IPs are capable of deprotonating alkynes was confirmed by reacting $\mathbf{1_H}$ with ∼10 equiv of phenylacetylene (Scheme 4a). Mixing both reagents in THF led to immediate formation of a yellow precipitate that is insoluble in both apolar and polar solvents. Attenuated total reflection infrared (ATR-IR) spectroscopy confirmed the presence of both polynuclear Cu^I(CCPh) and unreacted $\mathbf{1_H}$ (Figure S118), with no vibrations observed for a Cu(CCPh)(IP) species. At room temperature, the ^{1}H NMR spectrum of the *in vacuo* dried supernatant showed broad, uninformative resonances in the ^{1}H NMR spectrum (Figure S122), while the ^{31}P NMR spectrum (Figure S123) showed unreacted $\mathbf{1_H}$ (δ_P = 33.2 ppm). Cooling to −60 °C (Figures S124 and S125) led to the detection of $\mathbf{L1_H}$ and an additional resonance, which was identified as $((PPh_3)N(H)CH_2Ph)^+$, the conjugate acid of $\mathbf{L1_H}$ (δ_P = 38.6 ppm) (Figure S127). These resonances remain very broad, even at −60 °C, and are indicative of rapid exchange. No

https://dx.doi.org/10.1021/acs.organomet.0c00348
Organometallics 2020, 39, 3480−3489

Scheme 4. Overview of (Attempted) Synthetic Procedures to Prepare Catalytically Relevant Intermediates: (a) Reaction of $\mathbf{1_H}$ with Phenylacetylene; (b) Reaction of Copper Phenylacetylide with $\mathbf{L1_H}$; (c) Reaction of Copper Phenylacetylide with $\mathbf{L1_H}$ and Benzyl Azide

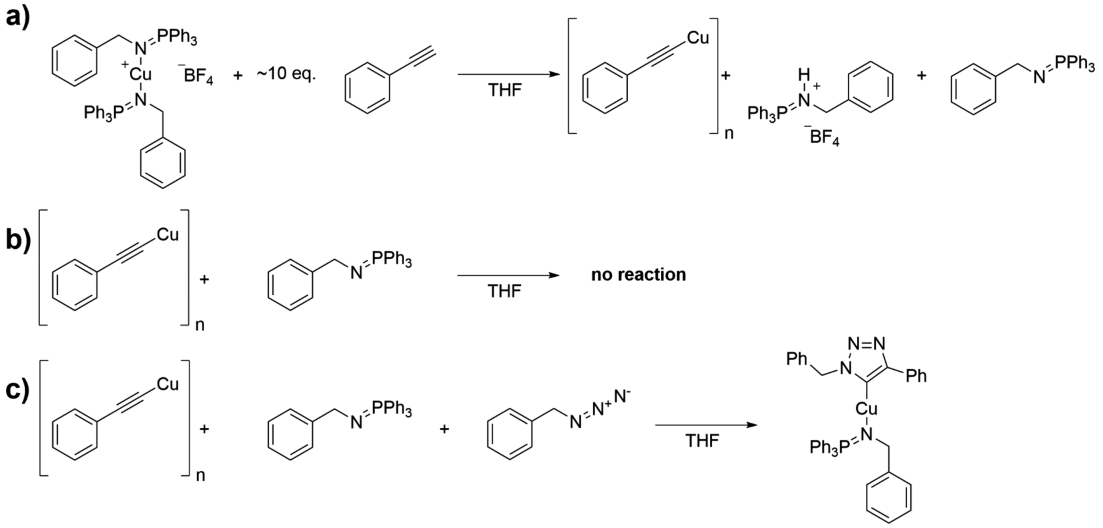

additional resonances were observed that could be assigned to a Cu(CCPh)(IP) species.

Other approaches that have been employed in the literature to prepare Cu phenylacetylide complexes include the direct reaction between polynuclear copper phenylacetylide and a suitable ligand.[30] However, a reaction to generate a well-defined species by mixing polynuclear copper phenylacetylide with $\mathbf{L1_H}$ to prepare Cu phenylacetylide was unsuccessful (Scheme 4b), with work-up only leading to quantitative isolation of both starting materials (Supporting Information, section 4.3). On the basis of the two previous unsuccessful reactions, we propose that monodentate IPs do not provide stable ligation to copper phenylacetylide.

During catalysis, the solution remains homogeneous, and no precipitation of polynuclear copper phenylacetylide species is observed. Combined with the observations made during the previous experiments (Scheme 4a,b), it is unlikely that the resting state during catalysis under the employed reaction conditions is a Cu acetylide complex. Another plausible candidate for the resting state is a Cu triazolide complex (Scheme 1). In this regard, recent DFT studies have shown that proton transfer from incoming acetylene substrate to a Cu triazolide species can become the rate-determining step if the alkyne is the only proton source present during the CuAAC reaction.[32]

To date, only a handful of Cu triazolide complexes have been isolated.[15,33−35] Common strategies to isolate such a copper triazolide complex involve reaction of a ligated Cu phenylacetylide complex with an organic azide. For our system, this approach is not viable as no ligated Cu phenylacetylide complexes could have been isolated. In an attempt to prepare the targeted Cu triazolide complex, a direct reaction was performed using Cu phenylacetylide, benzyl azide, and $\mathbf{L1_H}$ (Scheme 4c).

After work-up, an off-white solid was obtained that was sensitive to moisture and oxygen. The ^{1}H NMR spectrum is in line with the successful synthesis of Cu triazolide complex [Cu(PhCH$_2$N(PPh$_3$)(1-benzyl-4-phenyltriazolide)] ([Cu(triaz)($\mathbf{L1_H}$)]) (Figure 4), with a resonance at δ_H = 5.13 ppm that is not observed in $\mathbf{L1_H}$ or $\mathbf{1_H}$. This resonance is

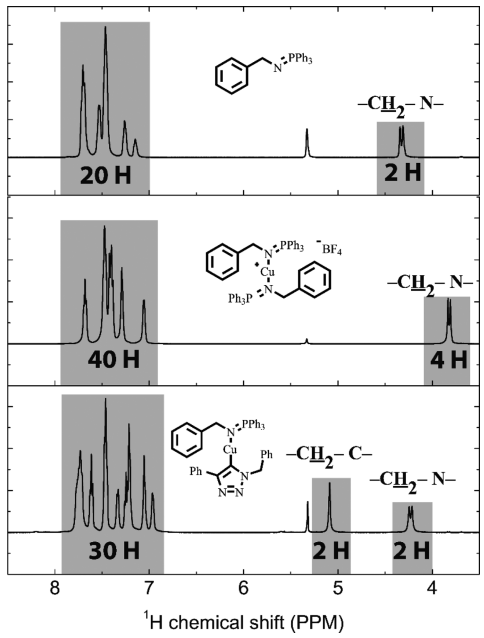

Figure 4. Comparison of the ^{1}H NMR spectrum of $\mathbf{L1_H}$ (top), $\mathbf{1_H}$ (middle), and [Cu(triaz)($\mathbf{L1_H}$)] (bottom) in CD_2Cl_2.

assigned to the benzylic hydrogens of the triazolide moiety. Additionally, the ^{13}C NMR spectrum shows two resonances (δ_C = 154.2 and 150.0 ppm) that can be attributed to the carbons of the C═C fragment present in the five-membered ring, in correspondence with data for an earlier isolated triazolide complex by Straub (δ_C = 154.6 and 152.2 ppm).[33] Finally, the ^{31}P NMR spectrum shows a single resonance at δ_P = 32.2 ppm.

The positive mode high-resolution CSI mass spectrum (Figure S101) shows the molecular ion peak for the homoleptic fragment [Cu((PPh$_3$)NCH$_2$Ph)$_2$]$^+$ (expected: 797.228; found: 797.224). Negative mode CSI HRMS (Figure S102) provides many fragments, including [Cu(triazolide)$_2$]$^-$ (expected: 531.136; found: 531.131).

https://dx.doi.org/10.1021/acs.organomet.0c00348
Organometallics 2020, 39, 3480−3489

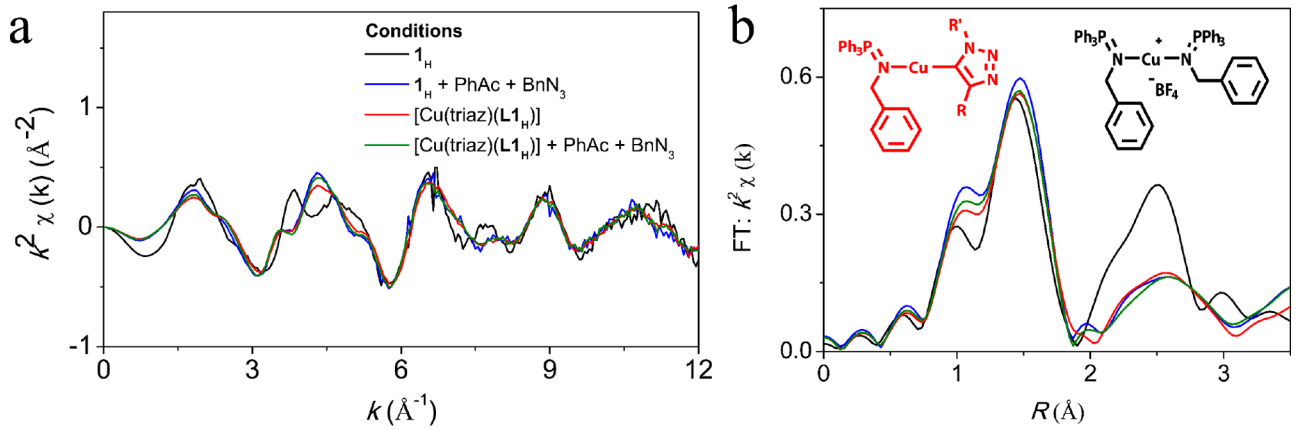

Figure 5. Comparison of the Cu K-edge XAS data for $\mathbf{1_H}$ and [Cu(triaz)($\mathbf{L1_H}$)] in the absence and presence of benzyl azide (1 equiv) and phenylacetylene (1.2 equiv). Under catalytic conditions, solutions were frozen after a reaction time of 10 min and 2.5 mol % of Cu was employed. Both samples were measured in THF. (a) k^2-weighted Cu K-edge EXAFS data. (b) Fourier transform of the Cu K-edge EXAFS data. For the Fourier transform, a k-range of 3−12 Å^{-1} was employed. (b) also shows structures of the corresponding complexes.

It is unclear whether the isolated complex is homoleptic or whether ligand exchange has occurred under MS conditions and the complex is heteroleptic. Of the few reported Cu triazolide complexes, none of them were homoleptic.[15,33−35] In addition, [Cu(triaz)($\mathbf{L1_H}$)] is highly soluble in toluene, deeming the formation of an ionic complex unlikely. Furthermore, the benzylic hydrogens of [Cu(triaz)($\mathbf{L1_H}$)] are significantly shifted compared to the benzylic hydrogens of $\mathbf{1_H}$, indicating a different chemical environment (Figure 4). On the basis of these findings, we propose that [Cu(triaz)($\mathbf{L1_H}$)] is indeed best formulated as a heteroleptic complex.

[Cu(triaz)($\mathbf{L1_H}$)] proved to be active in the CuAAC reaction between phenylacetylene (1.2 equiv) and benzyl azide (1 equiv) and showed similar activity compared to $\mathbf{1_H}$ (Figure S130). The similarity in catalytic activity of the two complexes suggests that the [Cu(triaz)($\mathbf{L1_H}$)] is indeed formed from the $\mathbf{1_H}$ system under catalytic conditions. Additional evidence for the formation of a Cu triazolide complex under catalytic conditions was found by using VT NMR and freeze-quench Cu K-edge EXAFS experiments. The ^{31}P NMR spectrum acquired at −50 °C shows two resonances at δ_P = 37.4 and 32.6 ppm (Figure S131), with the former signal being assigned to [$(PPh_3)N(H)CH_2Ph$]$^+$. The latter signal is very similar to the ^{31}P resonance as discussed previously for the Cu triazolide complex (Figure S97).

Furthermore, Cu K-edge EXAFS analysis of $\mathbf{1_H}$ reveals a Cu−N/Cu−C shell containing two atoms at a distance of 1.87(1) Å, a Cu−C shell containing six atoms at a distance of 2.90(2) Å, and a Cu−P shell containing two atoms at a distance of 3.03(1) Å (Figure 5 and Table 1). The bond distances and coordination numbers are in close agreement with the crystal structure of $\mathbf{1_H}$ (Figure 2). Under catalytic conditions, a solution containing the $\mathbf{1_H}$ complex shows a reduction of the coordination number of the Cu−P shell to one, in line with loss of one of the IP ligands. Also, the EXAFS analysis is in very close agreement with EXAFS analysis of [Cu(triaz)($\mathbf{L1_H}$)], providing further evidence for the formation of a Cu triazolide complex under catalytic conditions. Overall, the data support formulation of [Cu(triaz)($\mathbf{L1_H}$)] as the resting state during catalytic turnover in the CuAAC reaction, starting from $\mathbf{1_H}$. On the basis of the copper complex being two-coordinate, and on the absence of a Cu−Cu shell, we propose that the Cu triazolide complex is mononuclear.

Table 1. Cu K-Edge EXAFS Fitting Results for $\mathbf{1_H}$ and [Cu(triaz)($\mathbf{L1_H}$)] in THF in the Absence and Presence of Benzyl Azide and Phenylacetylene[a]

conditions[b]	coordination shell	σ^2 (Å^{-2})	d(Cu−X) (Å) exptl
$\mathbf{1_H}$	2 Cu−N	0.0037(7)	1.87(1)
	6 Cu−C	0.016(9)	2.90(2)
	2 Cu−P	0.005(2)	3.03(1)
$\mathbf{1_H}$ + PhAc + BnN_3[c,d]	2 Cu−C/ Cu−N	0.0022(6)	1.90(1)
	6 Cu−C	0.024(6)	3.03(3)
	1 Cu−P	0.003(2)	3.04(2)
Cu(triaz)($\mathbf{L1_H}$)	2 Cu−C/ Cu−N	0.0029(6)	1.89(1)
	6 Cu−C	0.022(5)	3.00(2)
	1 Cu−P	0.003(2)	3.02(2)
Cu(triaz)($\mathbf{L1_H}$) + PhAc + BnN_3[c,d]	2 Cu−C/ Cu−N	0.0028(5)	1.895(9)
	6 Cu−C	0.021(4)	3.02(2)
	1 Cu−P	0.003(1)	3.03(1)

[a]These parameters were used to obtain the fits shown in Figure 5. Fitting parameters without parentheses were kept fixed to reduce fitting parameters. Other fitting parameters are given in the Supporting Information. [b]2.5 mol % of Cu was used during catalytic experiments. [c]Reaction mixtures were frozen 10 min after mixing the reagents. [d]PhAc is used to denote phenylacetylene (1.2 equiv), and BnN_3 (1 equiv) is used to denote benzyl azide.

Having identified the resting state to be [Cu(triaz)($\mathbf{L1_H}$)], we performed kinetic experiments to investigate the pathway through which the triazole product is formed. First, the kinetic isotope effect (KIE) for deuterium-labeled phenylacetylene-d_1, determined by reacting phenylacetylene (0.6 equiv), phenylacetylene-d_1 (0.6 equiv), and benzyl azide (1 equiv) in the presence of $\mathbf{1_H}$ (2.5 mol %), was found to be 4.4(4) (Supporting Information, section 4.10), which shows that the mildly acidic C−H bond of phenylacetylene is broken in the rate-determining step.

Two pathways that are in agreement with this observation are depicted in Scheme 5. First, phenylacetylene may coordinate to the metal center and directly protonate the triazolide moiety to form the product and a copper−phenylacetylide complex. Second, proton transfer from phenyl-

https://dx.doi.org/10.1021/acs.organomet.0c00348
Organometallics 2020, 39, 3480−3489

Scheme 5. Hypothesized Pathways through Which the Product Triazole Is Formed[a]

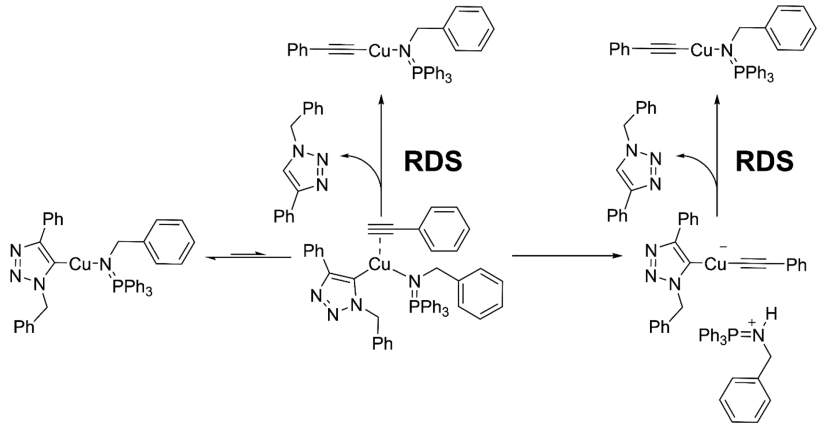

[a]Phenylacetylene can directly protonate the triazolide moiety to form the product. Alternatively, the ligand is first protonated and can then act as a proton shuttle. In this scheme, RDS is used to denote the rate-determining step.

acetylene to the basic IP ligand may precede protonation of the triazolide moiety, with IP acting as a proton shuttle.

To discern between the two pathways, we have reacted [Cu(triaz)(**L1**$_H$)] with phenylacetylene or $PhCH_2N(H^+)(PPh_3)BF_4$ for 2 h at room temperature. Both reactions lead to the triazole product, as evidenced by the ^{1}H NMR spectrum (Figure S138). If the ligand indeed does act as a proton shuttle, it should be beneficial for the catalytic activity to have additional $[PhCH_2N(H^+)(PPh_3)]BF_4$ present during catalysis. However, addition of $[PhCH_2N(H^+)(PPh_3)]BF_4$ (1 equiv) to [Cu(triaz)(**L1**$_H$)] had no effect on the catalytic performance compared to the standard conditions (Figure S139). These findings make it unlikely that catalysis occurs through proton shuttling facilitated by the IP ligand.

Next, we determined the order of the reaction with respect to copper and substrates (Table 2). A first-order dependency on the Cu concentration and a zeroth-order dependency in both substrates are observed when a large excess of both phenylacetylene and benzyl azide is used. The former indicates that a mononuclear Cu complex is involved in the rate-determining step or a dinuclear complex that stays intact in all stages of the catalytic cycle. Zeroth-order dependency on both substrates is indicative of saturation kinetics.[11]

Table 2. Overview of the Employed Conditions for the Order Determination of the Various Components of the 1$_H$ and [Cu(triaz)(L1$_H$)] System

component	Cu (equiv)	BnN_3 (equiv)[a]	PhAc (equiv)[b]	reaction order
Cu	1−3	225	205	1.1(1)
PhCCH	1	35	25−45	−0.02(7)
BnN_3	1	20−40	10	0.00(3)
PhCCH[c]	1	40	1−10	0.28(3)
BnN_3[c]	1	4−10	40	0.30(6)

[a]BnN_3 is used to denote benzyl azide. [b]PhAc is used to denote phenylacetylene. [c][Cu(triaz)(**L1**$_H$)] was employed due to the slow kinetics.

To limit saturation conditions, we reduced the amount of substrate with respect to the metal center. At low substrate concentrations, the formation of the Cu triazolide complex from **1**$_H$ was too slow for kinetic analysis. For this reason, we employed [Cu(triaz)(**L1**$_H$)] as the Cu source. For benzyl azide, a broken order of 0.30(6) is observed, and for phenylacetylene a broken order of 0.28(3) is observed. These broken orders indicate that phenylacetylene and benzyl azide are involved in a pre-equilibrium leading up to the rate-determining step(s).[36] A broken order with respect to phenylacetylene is in line with the KIE measurements and further confirms that coordination of phenylacetylene occurs during the rate-determining step(s).

A broken order with respect to benzyl azide also shows that benzyl azide coordination occurs during the rate-determining step(s). In line with the general mechanism of the CuAAC reaction (Scheme 1c), we propose that both the cyclization step and protonation step contribute to the overall rate of the reaction at low substrate loadings.

Evidence for coordination of a substrate was found in the Cu K-edge XANES region (Figure S117). Upon introduction of benzyl azide and phenylacetylene to a THF solution of [Cu(triaz)(**L1**$_H$)], a slight decrease in intensity of the pre-edge region is observed. The pre-edge region arises from 1s to 4p transitions; distortion from linearity gives rise to a decrease in intensity of the pre-edge region.[37] The slight decrease in intensity in the pre-edge region can be interpreted to arise from a small fraction of copper centers binding substrates (phenylacetylene or benzyl azide) under catalytic conditions.

Computational Study of the Cu Iminophosphorane System. To verify our experimental findings, we have performed DFT-D3 calculations at the BP86/TZ2P level of theory on the proposed catalytic cycle (Scheme 6) with the corresponding energies reported below the respective intermediates. The Cu triazolide complex, [Cu(triaz)(**L1**$_H$)] (**A1**), was used as a starting for the calculations.

Coordination of phenylacetylene to Cu triazolide **A1** yields Cu triazolide **A2**; this coordination step is mildly exergonic (ΔG° = −0.9 kcal mol^{-1}). Protonolysis of complex **A2** through reaction with phenylacetylene proceeds with a relatively high barrier (**TSA1**, $\Delta\Delta G^{\ddagger}$ = 22.5 kcal mol^{-1}) to yield the triazole and copper phenylacetylide complex **A3** ($\Delta\Delta G$ = 5.8 kcal mol^{-1}). **A3** is likely thermodynamically unstable, as no ligated copper phenylacetylide complex could be isolated.

A3 is incapable of directly coordinating benzyl azide. Instead, a rather large Cu−N distance (3.33 Å) is observed in the final geometry (**A4**, $\Delta\Delta G$ = −0.1 kcal mol^{-1}). Subsequent cycloaddition of benzyl azide and complex **A3** to yield six-membered cupracycle **A5** ($\Delta\Delta G$ = 7.9 kcal mol^{-1})

https://dx.doi.org/10.1021/acs.organomet.0c00348
Organometallics 2020, 39, 3480−3489

Scheme 6. (top) Proposed Catalytic Cycle for the CuAAC Reaction Catalyzed by Copper Iminophosphorane Complexes;[a] (bottom) Energy Diagram of the Proposed Catalytic Cycle with the Gibbs Free Energy Being Reported

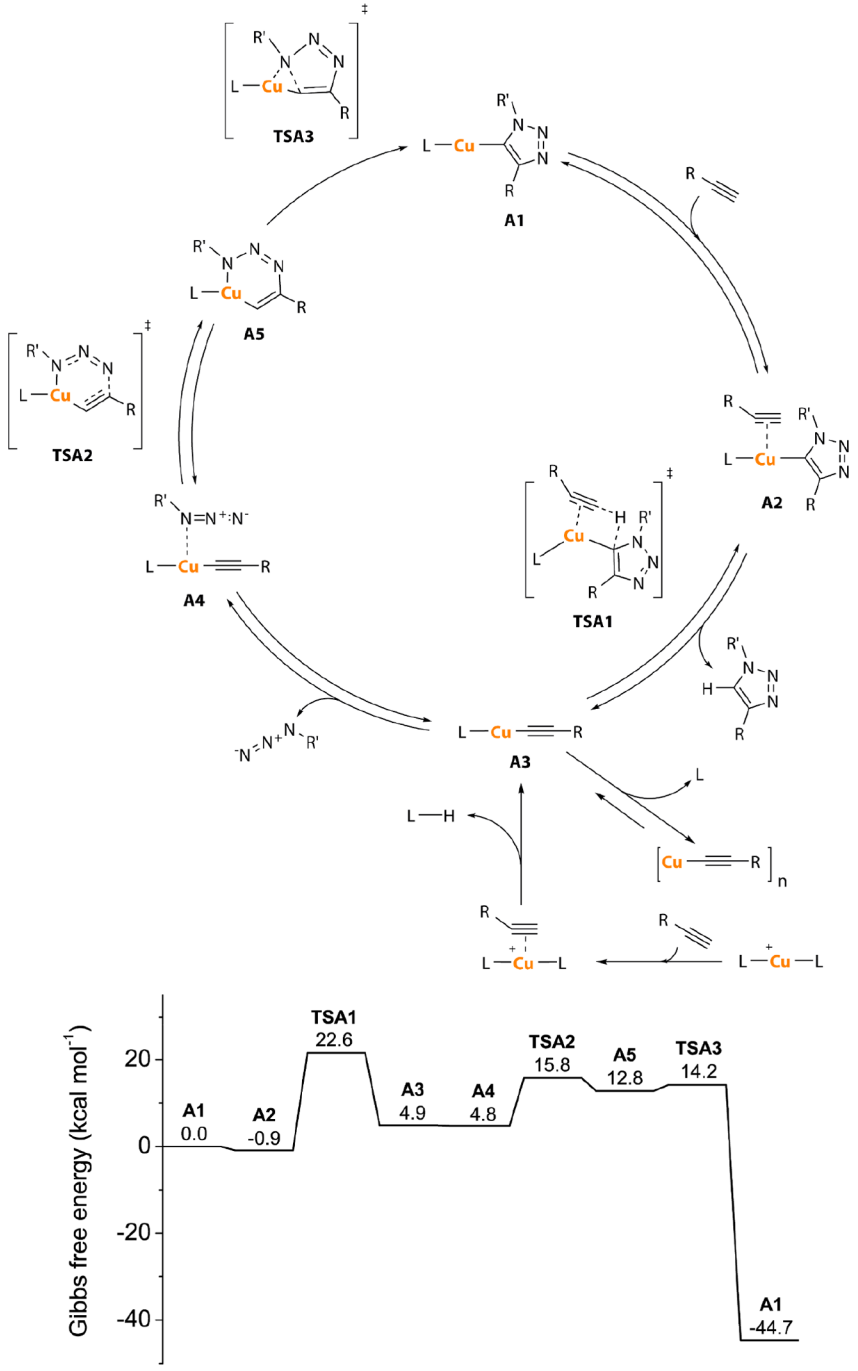

[a]DFT-D3 calculations were performed at the BP86/TZ2P level of theory. The R group denotes a phenyl substituent, and the R′ group denotes a benzyl substituent. The ligand (L) employed in these calculations was $PhCH_2N(PPh_3)$.

proceeds with a relatively low barrier (**TSA2**, $\Delta\Delta G^{\ddagger}$ = 11.0 kcal mol^{-1}). Ring contraction (**TSA3**, $\Delta\Delta G^{\ddagger}$ = 1.4 kcal mol^{-1}) of cupracycle **A5** to complete the cycle is highly exergonic ($\Delta\Delta G$ = −61.9 kcal mol^{-1}).

In line with our mechanistic studies, a rather small difference is observed between the barrier for protonation ($\Delta\Delta G$ = 5.8 kcal mol^{-1}, difference **TSA1** and **TSA3**). This difference is expected to be even smaller when (i) the polynuclearity of copper phenylacetylide is taken into consideration and (ii) the relative concentration of benzyl azide and phenylacetylene are taken into consideration (Table 2).[38]

These results are in line with both our experimental findings of a primary KIE for phenylacetylene and a broken order at low substrate loadings for both phenylacetylene and benzyl azide, given that both **TSA1** and **TSA3** likely contribute to the rate-determining step under these conditions. The intermediates and transition states proposed in this catalytic cycle are in close agreement with an early DFT study performed by Fokin and co-workers.[39] The authors, however, did not perform

https://dx.doi.org/10.1021/acs.organomet.0c00348
Organometallics 2020, 39, 3480−3489

calculations for the barrier of Protonolysis. The present study emphasizes that this barrier should also be taken into consideration, particularly under conditions where the alkyne is the proton source, to fully explain experimental observations.

As an alternative pathway, a mechanism proceeding through dinuclear intermediates was considered, but attempts to optimize dinuclear copper alkyne intermediates were hampered by the steric repulsion between the two copper complexes and a very large Cu−Cu distance (~5.00 Å), making a pathway proceeding via dinuclear intermediates unlikely. Besides, Cu−Cu scattering was not observed in our EXAFS analysis.

CONCLUSIONS

A mechanistic study of the CuAAC reaction, catalyzed by cationic copper iminophosphorane complexes, has been detailed in this work. Novel cationic, homoleptic Cu^{I} complexes ligated by iminophosphoranes were synthesized and fully characterized. All complexes showed to be active in the CuAAC reaction with model substrates benzyl azide and phenylacetylene. The observed activity trend $\mathbf{3}_{Cl} > \mathbf{1}_{H} > \mathbf{2}_{OMe}$ highlights the increased catalytic performance with increased Lewis basicity of the ligand.

Additionally, a Cu triazolide complex was prepared that was identified as the resting state in catalysis by spectroscopic and kinetic analysis. This Cu triazolide intermediate is proposed to be mononuclear based on Cu K-edge EXAFS analysis, kinetic analysis, and DFT calculations. Both protonolysis of the Cu triazolide and cyclization of Cu phenylacetylide intermediates contribute to the overall rate of the reaction, depending on the relative concentration of substrates. The spectroscopic and kinetic experiments were supplemented by DFT calculations to support the proposed catalytic cycle. This study shows that the use of weaker Lewis base ligands such as $\mathbf{3}_{Cl}$ catalysis is beneficial for the rate of reaction. Most likely, the activation barrier of protonolysis by phenylacetylene is lowered. The strong dependency on Lewis basicity could be applied in a more rational design of an efficient CuAAC catalyst employing, for example, carbenes.

EXPERIMENTAL SECTION

Experimental details are reported in the Supporting Information.

ASSOCIATED CONTENT

Supporting Information

The Supporting Information is available free of charge at https://pubs.acs.org/doi/10.1021/acs.organomet.0c00348.

Methods, synthetic procedures, XAS analysis, mechanistic investigations, and DFT coordinates (PDF)

X-ray crystallographic data (XYZ)

Accession Codes

CCDC 1979085−1979090 contain the supplementary crystallographic data for this paper. These data can be obtained free of charge via www.ccdc.cam.ac.uk/data_request/cif, or by emailing data_request@ccdc.cam.ac.uk, or by contacting The Cambridge Crystallographic Data Centre, 12 Union Road, Cambridge CB2 1EZ, UK; fax: +44 1223 336033.

AUTHOR INFORMATION

Corresponding Author

Moniek Tromp − *Sustainable Materials Characterization, Van't Hoff Institute for Molecular Sciences, University of Amsterdam, 1098 XH Amsterdam, The Netherlands; Materials Chemistry, Zernike Institute for Advanced Materials, University of Groningen, 9747 AG Groningen, The Netherlands;* orcid.org/0000-0002-7653-1639; Email: moniek.tromp@rug.nl

Authors

Bas Venderbosch − *Sustainable Materials Characterization, Van't Hoff Institute for Molecular Sciences, University of Amsterdam, 1098 XH Amsterdam, The Netherlands*

Jean-Pierre H. Oudsen − *Sustainable Materials Characterization, Van't Hoff Institute for Molecular Sciences, University of Amsterdam, 1098 XH Amsterdam, The Netherlands*

Jarl Ivar van der Vlugt − *Homogeneous, Supramolecular and Bio-Inspired Catalysis, Van't Hoff Institute for Molecular Sciences, University of Amsterdam, 1098 XH Amsterdam, The Netherlands*

Ties J. Korstanje − *Sustainable Materials Characterization, Van't Hoff Institute for Molecular Sciences, University of Amsterdam, 1098 XH Amsterdam, The Netherlands;* orcid.org/0000-0001-8036-5963

Complete contact information is available at: https://pubs.acs.org/10.1021/acs.organomet.0c00348

Author Contributions

B.V. and J.-P.H.O. contributed equally to this work.

Notes

The authors declare no competing financial interest.

ACKNOWLEDGMENTS

The authors thank NWO for funding (VIDI grant 723.014.010 (to M.T., B.V., and J.P.O.) and VENI grant 722.016.012 (to T.J.K.); the staff of the beamlines SuperXAS, Swiss Light Source (proposal numbers 20171764 and 20181154) in Villigen, Switzerland, and B18, Diamond Light Source (proposal number SP22432) in Didcot, UK, for support and access to their facilities; Josh Abbenseth for support during synchrotron measurements; and Jan-Meine Ernsting, Andreas Ehlers, and Ed Zuidinga for NMR spectroscopy and mass spectrometry support.

REFERENCES

(1) Kharb, R.; Sharma, P. C.; Yar, M. S. Pharmacological Significance of Triazole Scaffold. *J. Enzyme Inhib. Med. Chem.* **2011**, *26*, 1−21.

(2) Zhou, C.-H.; Wang, Y. Recent Researches in Triazole Compounds as Medicinal Drugs. *Curr. Med. Chem.* **2012**, *19*, 239−280.

(3) Huisgen, R. 1.3-Dipolare Cycloadditionen Rückschau Und Ausblick. *Angew. Chem.* **1963**, *75*, 604−637.

(4) Tornøe, C. W.; Christensen, C.; Meldal, M. Peptidotriazoles on Solid Phase: [1,2,3]-Triazoles by Regiospecific Copper(I)-Catalyzed 1,3-Dipolar Cycloadditions of Terminal Alkynes to Azides. *J. Org. Chem.* **2002**, *67*, 3057−3064.

(5) Rostovtsev, V. V.; Green, L. G.; Fokin, V. V.; Sharpless, K. B. A Stepwise Huisgen Cycloaddition Process: Copper(I)-Catalyzed Regioselective "Ligation" of Azides and Terminal Alkynes. *Angew. Chem., Int. Ed.* **2002**, *41*, 2596−2599.

(6) Kolb, H. C.; Finn, M. G.; Sharpless, K. B. Click Chemistry: Diverse Chemical Function from a Few Good Reactions. *Angew. Chem., Int. Ed.* **2001**, *40*, 2004−2021.

(7) Presolski, S. I.; Hong, V. P.; Finn, M. G. Copper-Catalyzed Azide-Alkyne Click Chemistry for Bioconjugation. *Curr. Protoc. Chem. Biol.* **2011**, *3*, 153−162.
(8) Touj, N.; Chakchouk-Mtibaa, A.; Mansour, L.; Harrath, A. H.; Al-Tamimi, J. H.; Özdemir, I.; Mellouli, L.; Yaşar, S.; Hamdi, N. Copper-Catalyzed Azide−Alkyne Cycloaddition (CuAAC) under Mild Condition in Water: Synthesis, Catalytic Application and Biological Activities. *J. Organomet. Chem.* **2017**, *853*, 49−63.
(9) Díez-González, S. Well-Defined Copper(i) Complexes for Click Azide-Alkyne Cycloaddition Reactions: One Click Beyond. *Catal. Sci. Technol.* **2011**, *1*, 166−178.
(10) Diez-Gonzalez, S. The Use of Ligands in Copper-Catalyzed [3 + 2] Azide-Alkyne Cycloaddition: Clicker than Click Chemistry? *Curr. Org. Chem.* **2011**, *15*, 2830−2845.
(11) Rodionov, V. O.; Fokin, V. V.; Finn, M. G. Mechanism of the Ligand-Free CuI-Catalyzed Azide-Alkyne Cycloaddition Reaction. *Angew. Chem., Int. Ed.* **2005**, *44*, 2210−2215.
(12) Ahlquist, M.; Fokin, V. V. Enhanced Reactivity of Dinuclear Copper(I) Acetylides in Dipolar Cycloadditions. *Organometallics* **2007**, *26*, 4389−4391.
(13) Worrell, B. T.; Malik, J. A.; Fokin, V. V. Direct Evidence of a Dinuclear Copper Intermediate in Cu(I)-Catalyzed Azide-Alkyne Cycloadditions. *Science* **2013**, *340*, 457−460.
(14) Makarem, A.; Berg, R.; Rominger, F.; Straub, B. F. A Fluxional Copper Acetylide Cluster in CuAAC Catalysis. *Angew. Chem., Int. Ed.* **2015**, *54*, 7431−7435.
(15) Jin, L.; Tolentino, D. R.; Melaimi, M.; Bertrand, G. Isolation of Bis(Copper) Key Intermediates in Cu-Catalyzed Azide-Alkyne "click Reaction. *Sci. Adv.* **2015**, *1*, No. e1500304.
(16) Chen, H.; Soubra-Ghaoui, C.; Zhu, Z.; Li, S.; Albright, T. A.; Cai, C. Isolation of an Acetylide-CuI3-Tris(Triazolylmethyl)Amine Complex Active in the CuAAC Reaction. *J. Catal.* **2018**, *361*, 407−413.
(17) Iacobucci, C.; Reale, S.; Gal, J.-F.; De Angelis, F. Dinuclear Copper Intermediates in Copper(I)-Catalyzed Azide-Alkyne Cycloaddition Directly Observed by Electrospray Ionization Mass Spectrometry. *Angew. Chem., Int. Ed.* **2015**, *54*, 3065−3068.
(18) Sun, S.; Wu, P. Mechanistic Insights into Cu(I)-Catalyzed Azide−Alkyne "Click" Cycloaddition Monitored by Real Time Infrared Spectroscopy. *J. Phys. Chem. A* **2010**, *114*, 8331−8336.
(19) Pérez-Balderas, F.; Ortega-Muñoz, M.; Morales-Sanfrutos, J.; Hernández-Mateo, F.; Calvo-Flores, F. G.; Calvo-Asín, J. A.; Isac-García, J.; Santoyo-González, F. Multivalent Neoglycoconjugates by Regiospecific Cycloaddition of Alkynes and Azides Using Organic-Soluble Copper Catalysts. *Org. Lett.* **2003**, *5*, 1951−1954.
(20) Lal, S.; Díez-González, S. [$CuBr(PPh_3)_3$] for Azide−Alkyne Cycloaddition Reactions under Strict Click Conditions. *J. Org. Chem.* **2011**, *76*, 2367−2373.
(21) Binauld, S.; Boisson, F.; Hamaide, T.; Pascault, J.; Drockenmuller, E.; Fleury, E. Kinetic Study of Copper(I)-catalyzed Click Chemistry Step-growth Polymerization. *J. Polym. Sci., Part A: Polym. Chem.* **2008**, *46*, 5506−5517.
(22) Qin, A.; Lam, J. W. Y.; Tang, L.; Jim, C. H. W.; Zhao, H.; Sun, J.; Tang, B. Z. Polytriazoles with Aggregation-Induced Emission Characteristics: Synthesis by Click Polymerization and Application as Explosive Chemosensors. *Macromolecules* **2009**, *42*, 1421−1424.
(23) All experiments were performed by using benzyl azide prepared from the same source of sodium azide as the catalytic activity was dependent on the choice of source of sodium azide. More details are reported in the Supporting Information (section 1.1).
(24) Binauld, S.; Fleury, E.; Drockenmuller, E. Solving the Loss of Orthogonality during the Polyaddition of α-Azide-ω-Alkyne Monomers Catalyzed by Cu(PPh3)3Br: Application to the Synthesis of High-Molar Mass Polytriazoles. *J. Polym. Sci., Part A: Polym. Chem.* **2010**, *48*, 2470−2476.
(25) Lal, S.; Rzepa, H. S.; Díez-González, S. Catalytic and Computational Studies of N-Heterocyclic Carbene or Phosphine-Containing Copper(I) Complexes for the Synthesis of 5-Iodo-1,2,3-Triazoles. *ACS Catal.* **2014**, *4*, 2274−2287.
(26) Cheisson, T.; Auffrant, A. Versatile Coordination Chemistry of a Bis(Methyliminophosphoranyl)Pyridine Ligand on Copper Centres. *Dalton Trans.* **2014**, *43*, 13399.
(27) García-Álvarez, J.; Díez, J.; Gimeno, J.; Suárez, F. J.; Vincent, C. (Iminophosphorane)Copper(I) Complexes as Highly Efficient Catalysts for 1,3-Dipolar Cycloaddition of Azides with Terminal and 1-Iodoalkynes in Water: One-Pot Multi-Component Reaction from Alkynes and in Situ Generated Azides. *Eur. J. Inorg. Chem.* **2012**, *2012*, 5854−5863.
(28) Semenov, S. N.; Belding, L.; Cafferty, B. J.; Mousavi, M. P. S.; Finogenova, A. M.; Cruz, R. S.; Skorb, E. V.; Whitesides, G. M. Autocatalytic Cycles in a Copper-Catalyzed Azide-Alkyne Cycloaddition Reaction. *J. Am. Chem. Soc.* **2018**, *140*, 10221−10232.
(29) Díez-González, S.; Nolan, S. P. [$(NHC)_2Cu$]X Complexes as Efficient Catalysts for Azide-Alkyne Click Chemistry at Low Catalyst Loadings. *Angew. Chem., Int. Ed.* **2008**, *47*, 8881−8884.
(30) de Boer, S. Y.; Gloaguen, Y.; Lutz, M.; van der Vlugt, J. I. CuI Click Catalysis with Cooperative Noninnocent Pyridylphosphine Ligands. Inorganica Chim. *Inorg. Chim. Acta* **2012**, *380*, 336−342.
(31) Núñez, M. G.; Farley, A. J. M.; Dixon, D. J. Bifunctional Iminophosphorane Organocatalysts for Enantioselective Synthesis: Application to the Ketimine Nitro-Mannich Reaction. *J. Am. Chem. Soc.* **2013**, *135*, 16348−16351.
(32) Özen, C.; Tüzün, N. Ş. Mechanism of CuAAC Reaction: In Acetic Acid and Aprotic Conditions. *J. Mol. Catal. A: Chem.* **2017**, *426*, 150−157.
(33) Nolte, C.; Mayer, P.; Straub, B. F. Isolation of a Copper(I) Triazolide: A "Click" Intermediate. *Angew. Chem., Int. Ed.* **2007**, *46*, 2101−2103.
(34) Winn, J.; Pinczewska, A.; Goldup, S. M. Synthesis of a Rotaxane Cu^{I} Triazolide under Aqueous Conditions. *J. Am. Chem. Soc.* **2013**, *135*, 13318−13321.
(35) Ziegler, M. S.; Lakshmi, K. V.; Tilley, T. D. Dicopper Cu(I)Cu(I) and Cu(I)Cu(II) Complexes in Copper-Catalyzed Azide−Alkyne Cycloaddition. *J. Am. Chem. Soc.* **2017**, *139*, 5378−5386.
(36) Kluwer, A. M.; Koblenz, T. S.; Jonischkeit, T.; Woelk, K.; Elsevier, C. J. Kinetic and Spectroscopic Studies of the [Palladium(Ar-Bian)]-Catalyzed Semi-Hydrogenation of 4-Octyne. *J. Am. Chem. Soc.* **2005**, *127*, 15470−15480.
(37) Kau, L. S.; Spira-Solomon, D. J.; Penner-Hahn, J. E.; Hodgson, K. O.; Solomon, E. I. X-Ray Absorption Edge Determination of the Oxidation State and Coordination Number of Copper. Application to the Type 3 Site in Rhus Vernicifera Laccase and Its Reaction with Oxygen. *J. Am. Chem. Soc.* **1987**, *109*, 6433−6442.
(38) Ryu, H.; Park, J.; Kim, H. K.; Park, J. Y.; Kim, S.-T.; Baik, M.-H. Pitfalls in Computational Modeling of Chemical Reactions and How To Avoid Them. *Organometallics* **2018**, *37*, 3228−3239.
(39) Himo, F.; Lovell, T.; Hilgraf, R.; Rostovtsev, V. V.; Noodleman, L.; Sharpless, K. B.; Fokin, V. V. Copper(I)-Catalyzed Synthesis of Azoles. DFT Study Predicts Unprecedented Reactivity and Intermediates. *J. Am. Chem. Soc.* **2005**, *127*, 210−216.

https://dx.doi.org/10.1021/acs.organomet.0c00348
Organometallics 2020, 39, 3480−3489